International Journal of Biological Macromolecules 354 (2026) 151321

Contents lists available at ScienceDirect

International Journal of Biological Macromolecules

journal homepage: www.elsevier.com/locate/ijbiomac

Palm oil improves UV-block, elongation, and water vapor resistance in biodegradable κ-carrageenan/starch films

Joice Camila Martins da Costa [a,*], Eloize da Silva Alves [a], Talita Aparecida Ferreira de Campos [a], Johny Paulo Monteiro [b], João Carlos Martins da Costa [c], Alessandro Francisco Martins [b,e], Tatiana La Banca Schreiner [d], Maria Filomena Filipe Barreiro [d], Elton Guntendorfer Bonafe [a,b,**]

[a] Laboratory of Food Chemistry, Postgraduate Program in Food Science, State University of Maringá, Maringá, PR, 87020-900, Brazil
[b] Laboratory of Materials, Macromolecules, and Composites (LaMMAC), Federal University of Technology – Paraná (UTFPR), Apucarana, PR, 86812-460, Brazil
[c] Federal University of Amazonas (UFAM), Manaus, AM, 69080-900, Brazil
[d] CIMO, LA SusTEC, Instituto Politécnico de Bragança, Campus de Santa Apolónia, 5300-253, Bragança, Portugal
[e] Department of Chemistry, Pittsburg State University, Pittsburg, 66762 KS, USA

ARTICLE INFO

Keywords:
Carotenoids
Sustainable
Polysaccharides
Active films

ABSTRACT

In view of the environmental contamination caused by plastic waste, this work proposes the development of sustainable and efficient active packaging based on κ-carrageenan/starch films added with palm oil. The films were produced by casting and extensively characterized. The incorporation of palm oil *via* emulsification resulted in a heterogeneous polysaccharide–lipid system, as evidenced by XRD, DSC, and SEM analysis. These structural rearrangements within the matrix led to higher localized organization. Consequently, the films exhibited enhanced mechanical and barrier performance. The formulation containing 1.5% palm oil exhibited 20% higher elongation than the control film (43.18% *vs.* 23.38%), and water vapor permeability reduced from 8.27×10^{-11} to 6.70×10^{-11} $g \times m^{-1} \times s^{-1} \times Pa^{-1}$. Furthermore, the presence of carotenoids in palm oil allowed the film to effectively block ultraviolet radiation, extending the shelf life of cherry tomatoes. The produced films not only demonstrated efficiency in UV blocking and improvements in mechanical and barrier properties, but also confirmed their biodegradability, with mass loss exceeding 50% within 60 days. In conclusion, the new polysaccharide-based active film, produced using sustainable, environmentally friendly technology, efficiently extends the shelf life of cherry tomatoes.

1. Introduction

Food packaging plays a fundamental role in the storage and distribution of products, protecting foods against external environmental factors and deterioration [1]. In recent years, growing concerns regarding environmental contamination caused by petrochemical-based plastics have driven an urgent search for sustainable and biodegradable alternatives [1–3]. In this context, packaging materials based on natural ingredients have been developed, using systems formulated with biomass such as polysaccharides [4], proteins [5], and lipids [6].

Among these materials, polysaccharides stand out because their combinations can result in materials with improved mechanical and barrier properties [7,8]. Starch is a widely available polysaccharide commonly used in food applications due to its non-toxicity and low cost [9]. However, starch-based materials often exhibit poor water resistance and mechanical fragility [10,11]. Starch limitations have been previously addressed by its combination with κ-carrageenan. Studies report that this coupling significantly enhances the physical and mechanical properties of the resulting material [12].

κ-Carrageenan is a polysaccharide extracted from red algae. It features a high molecular weight and a sulfated linear structure, which facilitates molecular interactions with the linear chains of starch. During solvent evaporation, this polymer promotes gel formation through a double-helix aggregation mechanism [9,10]. Consequently,

* Corresponding author.
** Correspondence to: E. Guntendorfer Bonafe, Laboratory of Food Chemistry, Postgraduate Program in Food Science, State University of Maringá, Maringá, PR, 87020-900, Brazil.
E-mail addresses: joicecamilamart@gmail.com (J.C.M. da Costa), eltonbonafe@utfpr.edu.br (E.G. Bonafe).

https://doi.org/10.1016/j.ijbiomac.2026.151321
Received 1 December 2025; Received in revised form 3 March 2026; Accepted 6 March 2026
Available online 7 March 2026

κ-carrageenan is widely used across various sectors, particularly the food industry. Its applications include edible films, texturizing agents, and encapsulation processes [13–15]. Furthermore, it is employed in the cosmetic, textile, pharmaceutical, and printing industries [16].

Despite their environmental benefits, the large-scale commercialization of biodegradable films remains limited. Conventional synthetic plastics remain highly competitive due to their ease of processing, biological inertness, and low production costs [17]. Nevertheless, studies show that consumers perceive biodegradable films and coatings as more sustainable alternatives to traditional plastic packaging. These materials are promising candidates for reducing single-use plastic consumption. Additionally, they extend food shelf life while preserving essential quality attributes [18].

In this context, active packaging has emerged as an innovative alternative to conventional options. These materials incorporate active agents that perform specific functions, such as antioxidant activity, UV radiation protection, or enhanced gas and water vapor barriers [10,11]. Although starch and κ-carrageenan films are environmentally sustainable, they often lack the functional properties of conventional active packaging. Recent studies have identified new functional activities in κ-carrageenan/starch blends [19–21]. These findings suggest significant potential for advancements in active packaging development.

Considering the incorporation of functional properties, various oils have been incorporated into film-forming mixtures to enhance barrier properties. Due to their hydrophobic nature and the presence of natural pigments such as carotenoids, these oils contribute to reducing water vapor permeability and blocking UV radiation, thereby slowing degradation processes and extending food shelf life [22,23]. Among the investigated oils, palm oil (PO) stands out as it is extracted from the ripe fruits of palm trees (*Elaeis guineensis*), presenting a reddish color, a balanced composition of saturated and unsaturated fatty acids, which contributes to protecting against UV radiation and contributes to food preservation [23,24]. Furthermore, PO is produced on a large scale, with approximately 90% of its production destined for the food industry, making it an attractive raw material for the development of food packaging materials [25,26]. Additionally, its incorporation may act as a plasticizer, improving the mechanical properties of the final material [27]. Glycerol is the most common plasticizer for polysaccharide-based films. It is produced on a large scale. Once purified, it is considered safe. The industry uses it widely in food, pharmaceuticals, and chemical additives [28].

Previous studies reported starch/κ-carrageenan [12] starch/κ-carrageenan loaded with zinc oxide nanoparticles [29], copper oxide nanoparticles [11], and extract of onion Skin [21]. However, no reports currently describe the development of starch/κ-carrageenan incorporating palm oil for food packaging. Thus, this study aimed to develop, characterize, and apply a novel active film composed of κ-carrageenan and starch incorporated with palm oil. The materials were prepared with different palm oil contents and characterized in terms of their physicochemical, mechanical, and barrier properties. Additionally, the biodegradability of the films was assessed under real disposal conditions. Their performance as active coatings were tested on fresh cherry tomatoes to evaluate their potential as sustainable food packaging.

2. Materials and methods

2.1. Materials

The materials used for film formation were: κ-carrageenan (molar weight of 277 kDa and CAS number 9000-07-1) donated by CP Kelco, Limeira, Brazil, cassava starch (amylose content 19%, donated by Indemil, Paranavaí, Brazil), glycerol (CAS number 56–81-5, Dinâmica, São Paulo, Brazil), Tween 80 M (weight of 1.31 kDa and CAS number 9005-65-6, Sigma-Aldrich, USA), and palm oil (Cepêra Alimentos, Salvador, Brazil). All the other reagents, such as anhydrous calcium chloride (molar weight of 110.98 g/mol and CAS number 10043–52-4, Êxodo Científica, São Paulo, Brazil) and magnesium nitrate (molar weight of 256.41 g/mol and CAS number 13446–18-9, Inlab, São Paulo, Brazil), were of analytical grade.

Table 1
Composition of the mixtures (100 mL) used to prepare films.

Films*	Glycerol (g)[a]/%	κ-carrageenan (g)/%	Starch (g)/%	Palm oil (mL)[b]/%	Tween 80 (mL)[c]/%
κ-0PO	1.50/50	2.25/2.25	0.75/0.75	0/0	0/0
κ-0.5PO	1.50/50	2.25/2.25	0.75/0.75	0.5/0.5	0.05/10
κ-1.0PO	1.50/50	2.25/2.25	0.75/0.75	1/1	0.10/10
κ-1.5PO	1.50/50	2.25/2.25	0.75/0.75	1.5/1.5	0.15/10

* The weight content of κ-carrageenan and cassava starch was expressed in w/v for 100 mL of the mixture. PO – palm oil.
[a] The concentration of glycerol was expressed in % w/w relative to the weight of polysaccharides in the mixture (100 mL).
[b] The palm oil % was based on the final mixture (100 mL).
[c] The tween 80 was added to 10% of the oil content. The films were prepared in triplicate ($n = 3$).

2.2. Preparation of the films

The films were prepared by casting [12] using the formulations presented in Table 1. Initially, cassava starch (1% *w/v*) and glycerol (50% *w/w*; polysaccharide - basis) were dissolved in distilled water (100.0 mL) under mechanical stirring (500 rpm). Subsequently, κ-carrageenan (2% w/v) was added, and the mixture was stirred for 15 min. The solution was then heated to 80 °C under continuous stirring until complete solubilization of the components (approximately 15 min). After that, the palm oil was emulsified (0.5, 1.0, and 1.5% *v/v*, filmogenic solution) using Tween 80 as the emulsifier (10% v/v, oil-basis). The film-forming solution was homogenized for 5 min at 12,000 rpm using a Ultra-turrax (IKA, T25, Brazil), poured into Petri dishes (150 mm × 15 mm), and dried in an oven at 40 ± 2 °C for 16 h. The films were labeled according to the amount of palm oil incorporated: κ-0PO, κ-0.5PO, κ-1PO, and κ-1.5PO. Digital images of the films were captured using a smartphone (Samsung, model A52S, Brazil).

2.3. Characterization of the emulsified palm oil

2.3.1. Dynamic light scattering (DLS)

The size distribution and zeta potential of palm oil droplets dispersed in the filmogenic solution were measured using a Dynamic Light Scattering (DLS) analyzer, Zetasizer model Nano ZS90 (Malvern Panalytical, UK). Prior to analysis, the solution was pre-dispersed in deionized water at a 1:1 (*v/v*) ratio and subjected to an ultrasonic bath at a frequency of 42 Hz for 1 min.

2.4. Characterization of the κ-carrageenan/starch films

2.4.1. Fourier transform infrared spectroscopy (FTIR)

The infrared spectra of the precursors and films were obtained using a Fourier-Transform Infrared (FTIR) spectrometer, model Cary 360 (Agilent Technologies, USA), operating in Attenuated Total Reflectance (ATR) mode. Data were collected over the 4000–400 cm^{-1} range, with 64 scans and a resolution of 4 cm^{-1}.

2.4.2. Scanning electron microscopy (SEM)

The surface morphology of the films was evaluated using a Scanning Electron Microscope (SEM) model JEOL JSM-5600LV (Japan). The samples were mounted on circular aluminum stubs and coated with a thin layer of gold. Micrographs were captured at an accelerating voltage of 5 kV and a working distance of 11 mm.

2.4.3. Differential scanning calorimetry (DSC)

The thermal properties of the films were analyzed using a

Differential Scanning Calorimeter (DSC) (Shimadzu DSC-60 Plus, Japan) [30]. The DSC analysis was carried out between 20 and 300 °C, at a heating rate of 10 °C/min under a constant argon flow of 50 mL/min.

2.4.4. X-ray diffraction (XRD)

X-ray diffraction (XRD) analysis of the films was performed using a Shimadzu diffractometer, model 7000 (Japan). Diffraction patterns were obtained using Cu Kα radiation (0.154 nm) at an accelerating voltage of 40 kV and a current of 30 mA. Data were collected over a 2θ range of 10° to 80°, with a scanning rate of 5°/min.

2.5. Mechanical properties

The mechanical properties were evaluated according to a previous study [11]. The parameters tensile strength (σ – MPa), elongation at break (ε – %), and Young's modulus (E – MPa) were measured using a texture analyzer (Stable Micro Systems, TA.XT Plus model, UK). Film samples (7 cm × 1 cm) were tested at a speed of 1 mm/s over a maximum distance of 100 mm. Mechanical parameters were determined based on five replicates. The thickness of the specimens was measured using a digital micrometer (YST Tech, YUANLS-H4024) with an accuracy of 0.001 mm and a measurement range of 0–25 mm. Mean thickness values were estimated from fifteen random measurements.

2.6. Water vapor permeability (WVP)

Water vapor permeability (WVP) measurements were performed according to the ASTM E-96 (2000) standard with modifications [31]. Initially, the materials were cut into circular samples (d = 60 mm) and conditioned for 48 h in a desiccator at 25 ± 2 °C at 53% relative humidity (saturated calcium chloride solution). The samples were then sealed over the opening of a permeation cell filled with magnesium chloride (33% relative humidity). The cell was transferred to a desiccator containing sodium chloride (75% relative humidity), resulting in a relative humidity gradient of 42%. Water vapor transmission rate (WVTR) was determined from the weight gain over 24 h $\left(\frac{m}{t}\right)$. Both WVTR and WVP were calculated using Eqs. 1 and 2.

$$\mathrm{WVPR} = \frac{\Delta m}{A \times \Delta t} \tag{1}$$

$$\mathrm{WVP} = \frac{WVPR \times \ X}{\Delta P} \tag{2}$$

where Δm is the change in mass for 24 h (t), A is the permeation area (m^2), X is the film thickness (mm), and ΔP is the water vapor pressure difference across the two sides of the film (Pa).

2.7. Moisture content

Moisture content was determined according to Bruni et al. [29]. Previously calcined porcelain crucibles containing films (2 cm × 2 cm) were weighed (M_1) and placed in a forced-air oven at 103 ± 2 °C until constant weight (M_2). Moisture content (%) was calculated using Eq. 3.

$$\mathit{Moiusture}\ (\%) = \frac{(M_1 - M_2)}{M_1} \times 100 \tag{3}$$

where M_1 and M_2 are the initial and final mass of the materials, respectively.

2.8. Swelling degree

The swelling degree was determined according to Berton et al. [32] with modifications. Dried films M_d (2 cm × 2 cm) were immersed in Falcon tubes containing 30 mL of distilled water and shaken at 100 rpm for 24 h. After this period, the swollen samples were removed and weighed M_i. The swelling degree was calculated using Eq. 4.

$$\mathit{Swelling\ Degree}\ (\%) = \frac{M_i - M_d}{M_i} \times 100 \tag{4}$$

where M_d and Mi are the mass of the film before and after swelling, respectively.

2.9. Oil permeability

Oil permeability was determined according to the method described by Bruni et al. [29]. For that, the films were cut into circular shapes (d = 2 cm) and placed on top of cylindrical glass vials containing 5 mL of soybean oil. The films were secured using perforated screw caps. The vials were then inverted into pre-weighed filter papers and placed in a desiccator at 25 °C for 48 h. After this period, the filter papers were removed and weighed. Oil permeability through films was calculated using Eq. 5.

$$\text{Oil Permeability} = \frac{\Delta W \times X}{A \times t} \tag{5}$$

where, ΔW The difference in filter paper mass, X is the film thickness (mm), A is the exposed area (m^2), and t is the analysis time (days).

2.10. Optical measurements

The color parameters lightness/brightness (L), redness/greenness (a), and yellowness/blueness (b*), as defined by the Commission Internationale de l'Éclairage (CIE), were determined using a digital colorimeter (Minolta, CR-400, Japan). The equipment was calibrated according to the manufacturer's instructions. Measurements were performed in triplicate. The whiteness index (WI), yellowness index (Y*i*), and total color difference (ΔE) were calculated using Eqs. 6, 7, and 8.

$$\mathrm{WI} = 100 - \sqrt{(100 - L)^2 + a^2 + b^2} \tag{6}$$

$$\mathrm{Y}i = 100 - \sqrt{(100 - L)^2 + a^2 + b^2} \tag{7}$$

$$\Delta\mathrm{E} = \sqrt{(L^* - L)^2 + (a^* - a)^2 + (b^* - b)^2} \tag{8}$$

where L* (97.54), a*(−0.03), and b* (1.79) were the standard parameters obtained from the white color plate.

The films, cut into rectangular dimensions (4 cm × 1 cm), were analyzed in triplicate using a spectrophotometer (Thermo Fisher Scientific, Genesys 10-S). Apparent opacity and UV barrier properties were determined at 550 nm and 280 nm, respectively. Opacity was calculated according to Eq. 9.

$$\mathit{Opacidade} = \frac{Abs_{550}}{X} \tag{9}$$

where Abs_{550} corresponds to the absorption at 550 nm and X is the thickness of the film (μm).

2.11. Total carotenoid content

The total carotenoid content in the films was determined based on previous studies [33] with adaptations. The films (5 g) were washed with 15.0 mL of isopropyl alcohol and 5 mL of hexane, stirred on a magnetic stirrer for 5 min, and transferred to a separatory funnel containing 85.0 mL of distilled water. After 30 min, the lower phase was discarded, and the upper phase was rewashed with two portions of 85.0 mL of distilled water. The supernatant was transferred to a volumetric flask (50 mL) containing 5 mL of acetone and brought to volume with hexane. Absorbance readings were performed at 450 nm using a spectrophotometer (Genesys 10-S UV/Vis, Rochester, USA). The blank

solution was prepared by acetone and hexane (1:9). The total carotenoid content (mg/100 g) was calculated using Eq. 10.

$$\text{CT (mg/100g)} = \frac{Abs_{440} \times 100}{250 \times a \times b} \quad (10)$$

where a is the cuvette path length (cm), and b is the ratio between the initial sample mass (5 g) and the final dilution volume (50 mL).

2.12. Coating performance on fresh fruits

The materials were evaluated as coatings applied to cherry tomatoes. Fresh fruits at a uniform ripening stage (pre-ripening) were purchased from a local market in the city of Maringá, Paraná, Brazil (23° 25′ 31″ S / 51° 56′ 19″ W). After sanitization in a sodium hypochlorite solution (0.1 g/L) for 10 min, the tomatoes were rinsed with distilled water and dried with paper towels. Subsequently, the tomatoes were immersed in the film-forming solution for 30 s and placed on racks for drying. The coated fruits were stored in a biochemical oxygen demand (B.O.D.) incubator (SolidSteel, São Paulo, Brazil) under controlled conditions of temperature (25 ± 0.5 °C) and relative humidity (66%). The performance was conducted with uncoated fruits (control) and fruits coated with no palm oil (κ-0PO) or with palm oil (κ-1.5PO) for 10 days. Shelf life was monitored four times (1, 3, 7, and 10 days) through digital imaging, weight loss, titratable acidity, and pH [34,35].

2.12.1. Weight change

The tomatoes were weighed at different intervals (1, 3, 7, and 10 days). The analyses were performed in triplicate, and mass loss was determined based on Eq. 11.

$$\textit{Weight change}\ (\%) = \frac{(Wo - Wf)}{Wf} \times 100 \quad (11)$$

where Wo indicates the initial weight and Wf the final weight.

2.12.2. Titratable acidity content

Titratable acidity was determined using 5 g of pulp diluted in 50 mL of distilled water. A 25,0 mL aliquot was then titrated with 0.1 mol/L NaOH. The endpoint was identified by the persistent color change of phenolphthalein. The results were calculated according to Eq. 12.

$$\textit{Acidity}\ (\%) = \frac{Vol_{NaOH} \times N_{NaOH} \times P \times W_{eq}}{W} \quad (12)$$

where P is the number of dilutions, Weq is the equivalent weight of citric acid, N_{NaOH} is the normality of NaOH, and W is the sample weight. All measurements were performed in triplicate.

2.12.3. pH measurement

The pH was measured in 5 g of crushed tomato using a calibrated benchtop pH meter (LUCA-210 P). Measurements were performed in triplicate.

2.13. Biodegradability

The biodegradability of the films was evaluated according to a previous study [36] with modifications. Dried film samples (2 × 2 cm^2) were fixed to a mesh screen and buried 15 cm below the soil surface. At different time intervals, the films were carefully retrieved, cleaned, and dried at room temperature for subsequent weighing. The biodegradation process was monitored by measuring the mass loss of the materials.

2.14. Statistical analysis

The data obtained were subjected to analysis of variance (ANOVA), and mean comparisons were performed by Tukey's test at a 95% confidence ($p \leq 0.05$), using STATISTICA software version 7.0 (STATSOFT Inc., São Paulo, Brazil).

Fig. 1. Digital images of the κ-carrageenan/starch films. PO – palm oil.

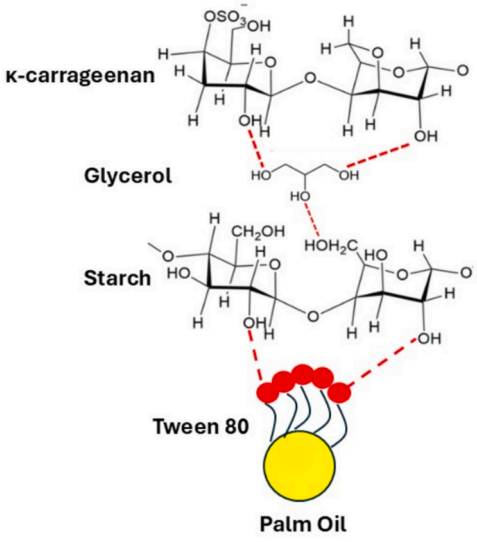

Fig. 2. Schematic formation of κ-carrageenan/starch/palm oil films.

3. Results and discussion

3.1. Development of the κ-carrageenan/cassava film

κ-carrageenan/cassava starch-based films were functionalized with PO. The original formulation of the active films followed previous studies [12]. PO was incorporated into the film through emulsification in the filmogenic solution. κ-carrageenan acts as a reinforcing agent for starch macromolecules. The predominantly linear structure of this sulfated polysaccharide interacts synergistically with the starch matrix, resulting in a composite material with enhanced mechanical performance. When plasticized with glycerol, both components function effectively as emulsion stabilizers, facilitating improved interactions with the linear segments of starch macromolecules. According to Karbowiak et al. [37], charged polysaccharides such as carrageenan exhibit pronounced polyelectrolyte behavior due to the presence of sulfate

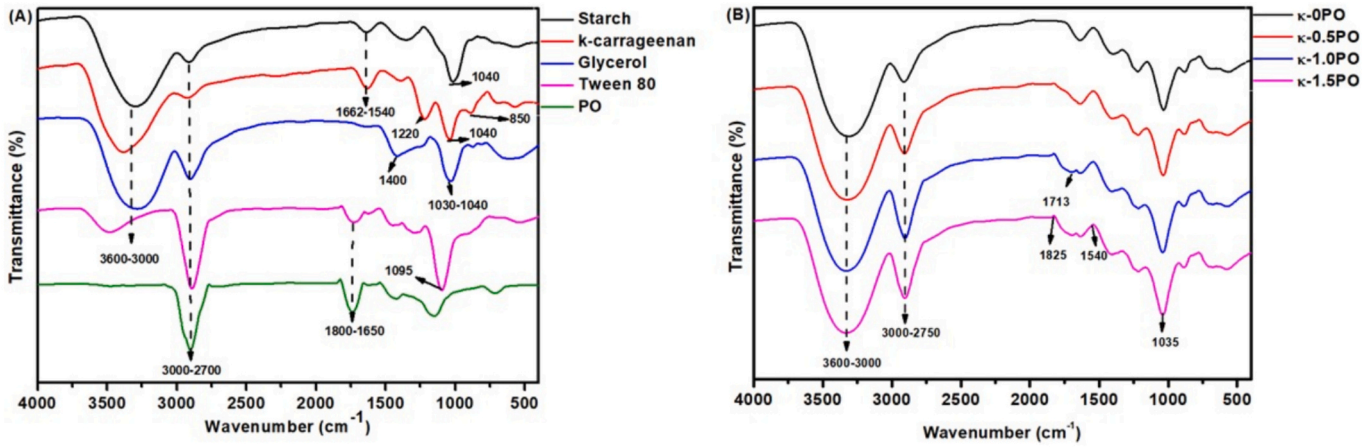

Fig. 3. FTIR spectra: (A) film forming precursors and (B) κ-carrageenan/starch films.

groups. As a result, these biopolymers can interact with a variety of components, including lipids and other additives.

Digital images of the control and enriched films containing 0.5, 1.0, and 1.5% (*w/v*) of PO are shown in Fig. 1. The films display a homogeneous surface, no visible bubbles or cracks after drying. The apparent stability of the films, as evidenced by the images, was maintained in the PO-containing materials. It was corroborated by Dynamic Light Scattering (DLS). Particle sizes of 339.1 nm (κ-0PO), 610.04 nm (κ-0.5PO), 542.6 nm (κ-1.0), and 369.1 nm (κ-1.5) display zeta potential of −48.3, −59.0, −60.2, and − 64.0 mV, respectively.

A recent study attributed high colloidal stability to droplets with zeta potentials above +30 mV or below −30 mV. The strong electrostatic repulsion among the negatively charged droplets effectively prevented their coalescence [11,38]. The resulting negative charge on the droplet likely originates from $–SO_3^-$ groups (identified by FTIR, section 3.2) of κ-carrageenan; the κ-carrageenan/starch ratio of 2:1 supports this. A schematic representation of the formation of the active κ-carrageenan/starch/palm oil films is shown in Fig. 2.

The PO content was found to be significant, with the sample loaded with 1.5% PO. Those outcomes are in line with L'Estimé and co-workers [39]. Increasing the oil content in the dispersed phase increases the emulsion's viscosity. The increased viscosity enables more intense, uniform energy transmission throughout the system during agitation. As a result, droplets deform and break into smaller particles when the stress from the continuous phase exceeds the interfacial tension of the dispersed phase.

3.2. Fourier transform infrared spectroscopy (FTIR)

The FTIR spectra of precursor materials and films are shown in Fig. 3. The spectra of starch, κ-carrageenan, glycerol, and Tween 80 display a band between 3600 and 3000 cm^{-1}, attributed to O—H stretching and hydrogen-bonding interactions [11]. Signals between 2700 and 3000 cm^{-1} correspond to aliphatic –CH stretching vibrations [40,41], particularly for Tween 80 and PO. Bands between 1662 and 1540 cm^{-1}, observed in the spectra of starch and κ-carrageenan, are associated with polymer–water interactions of C—O groups [42,43]. Signals at 1220 and 850 cm^{-1} are assigned to the S═O do $–SO_3^-$ and the galactose-4-sulfate repeat unit, both from κ-carrageenan [12]. PO and Tween 80 exhibit a band between 1650 and 1800 cm^{-1}, assigned to carbonyl of ester C═O stretching and C═C double-bond vibrations [44,45]. Only Tween 80 presents a strong peak at 1095 cm^{-1}, related to C—O stretching vibrations [46].

The spectra of the control films and the films with palm oil exhibited similar peaks. However, the amplitudes around 1825–1540 cm^{-1} varied according to the palm oil content. This similarity is mainly observed in the regions between 3600 and 3000 cm^{-1} and 3000–2700 cm^{-1} is related to O—H stretching [11] and asymmetric and symmetric stretching of aliphatic C—H (CH_2 and CH_3 groups) [40,41]. While the vibration at 1030–1040 cm^{-1} and 1400 cm^{-1} are assigned to the C—O of

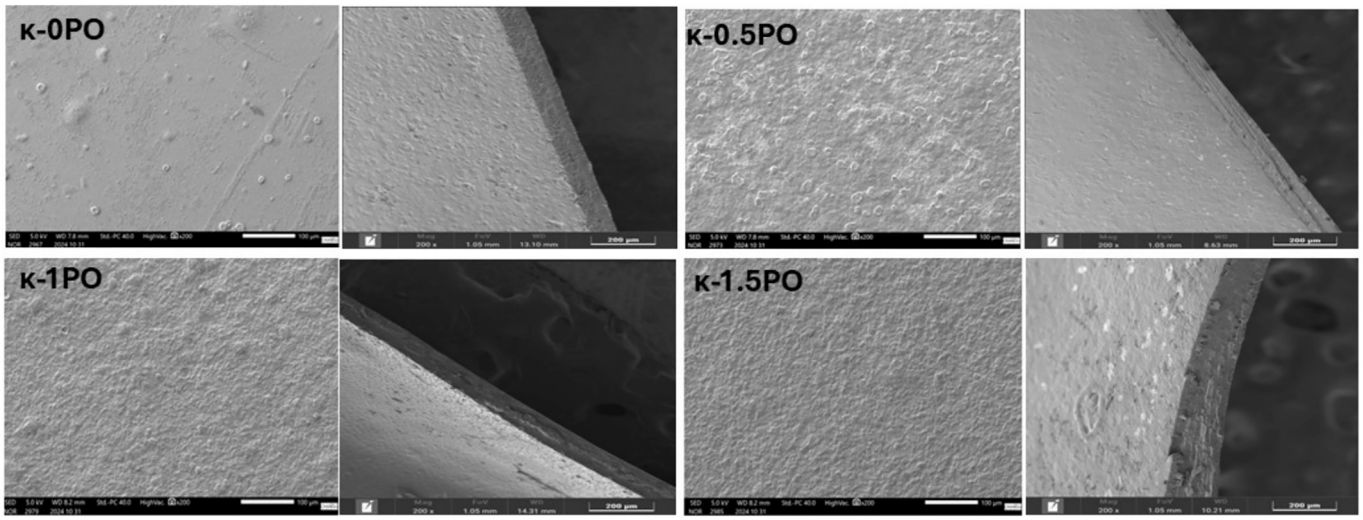

Fig. 4. SEM micrographs of the κ-carrageenan/starch films.

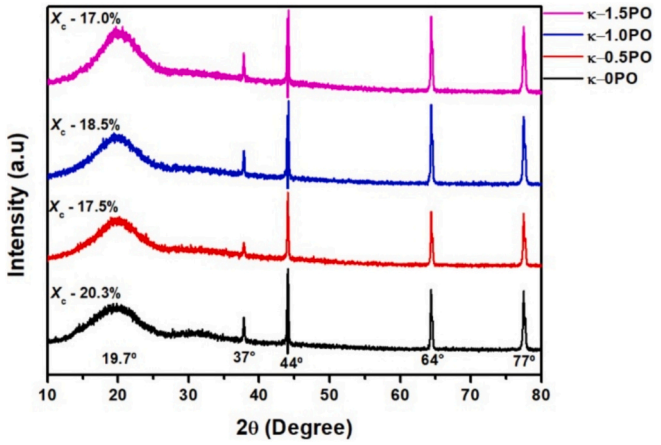

Fig. 5. XRD patterns of κ-carrageenan/starch films.

primary and secondary alcohols, and O—H bending of angular deformation of hydroxyl groups, respectively. However, the addition of Tween 80 and PO produced changes in the regions where ester groups absorb (~1825–1540 cm^{-1}) [47]. Gelatin-based films enriched with PO support these findings [48]. Spectral modifications are noticeable in samples containing 1.0 and 1.5% (*w/v*) of PO.

3.3. Scanning electron microscopy (SEM)

Surface and cross-sectional scanning electron microscopy (SEM) micrographs of the films are presented in Fig. 4. The addition of PO altered the film matrix surface. The micrographs display visually distinct surfaces under the same magnification. The control film exhibits a mostly smooth surface, whereas roughness predominates in the PO-containing films. Although the surfaces are different (control and PO-loaded films), the cross-sectional micrographs revealed internal structure kept regular. The tortuosity observed on the surface of PO-loaded films may be due to oil droplets that form during drying. Previous studies suggest that lipophilic microdomains formed on the surface modify surface topography and act as physical barriers to gas permeation [49]. Pectin/carboxymethylcellulose-based films loaded with citrus essential oil show similar behavior. The authors reported that droplet flocculation and aggregation during film preparation and drying are responsible for these surface changes [50]. Gellan gum (0.05% *w/v*) films emulsified with 18% (*w*/w) Tween 80 and loaded with palm kernel oil exhibit the same pattern [51].

3.4. X-ray diffraction (XRD)

The XRD patterns of κ-carrageenan/starch films with different concentrations of palm oil are presented in Fig. 5. The diffractograms display amorphous regions at 2θ (10–35°) and crystalline peaks at 2θ (37°, 44°, 64°, and 77°). The crystallinity index obtained from the ratio between crystalline and amorphous–crystalline areas confirm the amorphous nature of the material. However, the PO addition to the mixture induced internal structural changes in the films. The comparison of the crystallinity index (Xc, %) between the control and PO-films supports this observation. The control films exhibited higher Xc values than the materials containing 0.5, 1.0, and 1.5% PO.

These outcomes suggest partial structural reorganization of the matrix at higher lipid contents. This behavior may be related to localized packing of lipid domains and to rearrangements of polysaccharide chains driven by polymer–lipid interactions. Importantly, these changes did not compromise the predominantly amorphous nature of films. The micrographs further support these findings, revealing clear differences between control and PO-loaded films. Lee et al. [52] reported biodegradable films based on bean starch and guar gum (4% *w*/w) loaded with 0, 0.5, 1.0, and 2.0% (*w*/w) sunflower oil. The addition of sunflower oil resulted in a less crystalline structure, attributed to a reduction in intermolecular forces between the polysaccharide chains.

3.5. Differential scanning calorimetry (DSC)

The Differential Scanning Calorimetry (DSC) curves of the films are shown in Fig. 6. The materials exhibited exothermic peaks between 216 and 236 °C. The results indicate degradation occurring at different temperatures, suggesting internal structural changes within the material. Increasing the PO content decreased the event temperature. The κ-0PO required approximately 20 °C higher temperature to produce the same thermal event as the sample with the highest PO content (κ-1.5PO). Thus, more organized materials, with better chain-to-chain packing, require greater energy to break the interactions holding them together. These findings are consistent with the XRD results.

Tongnuanchan et al. [49] produced biodegradable films composed of 3.5% (*w/v*) gelatin plasticized with 35% (w/w) glycerol and enriched

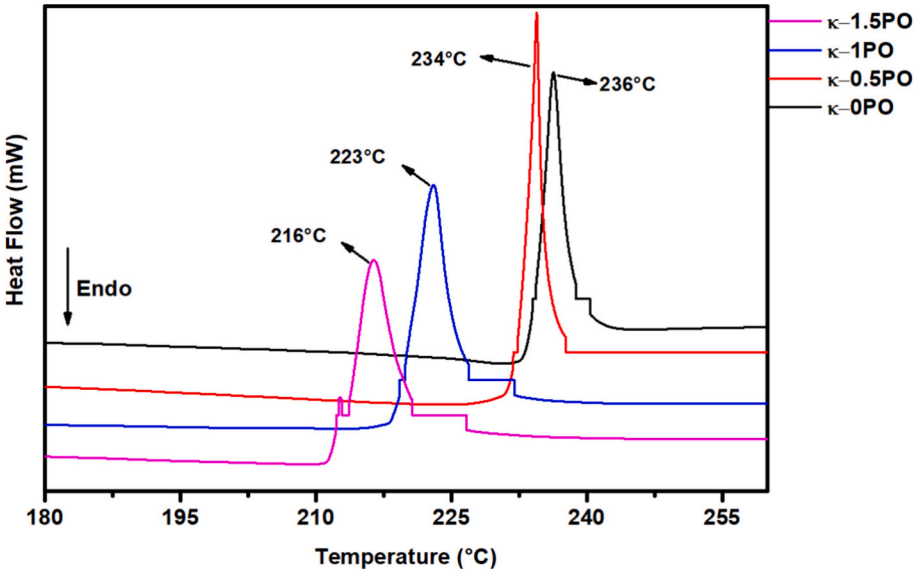

Fig. 6. DSC curves of κ-carrageenan/starch films.

Table 2
Thickness, mechanical properties, and water vapor permeability of the κ-carrageenan/starch films.

Films	κ-0PO	κ-0.5PO	κ-1PO	κ-1.5PO
Thickness (μm)	100 ± 0.10^{d}	130 ± 0.10^{c}	150 ± 0.00^{b}	160 ± 0.10^{a}
σ (MPa)	1.10 ± 0.01^{c}	1.00 ± 0.00^{c}	1.70 ± 0.00^{a}	1.20 ± 0.00^{b}
ε (%)	23.38 ± 1.18^{d}	34.39 ± 1.11^{c}	37.40 ± 2.94^{b}	43.18 ± 4.31^{a}
E (MPa)	0.002 ± 0.00^{b}	0.003 ± 0.00^{a}	0.003 ± 0.00^{a}	0.001 ± 0.00^{c}
WVP (10^{-11})(g × m^{-1} × s^{-1} × Pa)	8.27 ± 1.04^{c}	9.62 ± 1.22^{a}	9.01 ± 1.17^{b}	6.70 ± 1.72^{d}

Results are presented in (mean ± standard deviation); $n = 3$. WVP: water vapor permeability; σ (MPa) Tensile strength; ε (%): Elongation at break; E (MPa): Young's modulus. a, b, c, d Different letters in the same line indicate significant differences ($p \leq 0.05$) according to Tukey's test.

with palm oil at 25, 50, 75, and 100% (w/w) of the polymer. The authors reported similar results. Increasing the palm oil content in the blend reduced the temperature of thermal events compared to the control film. The interaction between emulsion droplets and polymer chains disrupts chain-to-chain interactions. The authors reported that this disruption increases the free volume between polymer chains, thereby enhancing mobility within the film matrix [49]. Moreover, Shamsuri and Jamil [53] reported that the addition of lipid fluids disrupts chain-to-chain interactions, reducing the energy required to break the intermolecular connections.

3.6. Thickness, mechanical properties, and water vapor permeability

The thickness of the materials is an important parameter for estimating barriers and mechanical properties. Measurements were performed for all samples, showing an increase in value with the addition of PO (Table 2). Thus, the internal changes caused by incorporating PO through emulsification support these findings [54,55]. According to a previous study, films with thicknesses between 80 and 200 μm are suitable for packaging or coating applications [43]. Therefore, all formulations meet the application criteria, ranging from 100 ± 0.10 μm to 160 ± 0.10 μm. Commercial materials based on low-density polyethylene and polypropylene typically range between 15 and 250 μm and 12–125 μm, respectively [56].

The mechanical properties of the films were estimated from the stress–strain curves, including tensile strength (σ), elongation at break (ε), and Young's modulus (E). Notably, the addition of PO led to significant changes in the materials' mechanical behavior. The essential oil acted as a plasticizer in the blend. The elongation at break value indicates increased elasticity as PO levels rose in the formulations. The κ-1.5PO material exhibited the highest ε value, approximately 20% higher than that of the control film (κ-0PO). The weakening of chain-to-chain interactions caused by the plasticizing effect of PO is supported by the low Young's modulus (0.001–0.003 MPa) and tensile strength (1–1.7 MPa) values. The incorporation of lipids in polysaccharide-based films can increase matrix flexibility and contribute to improved tensile performance, resulting in a more stable film system [57]. The XRD results are also consistent with the mechanical data, indicating that PO incorporation led to less-organized materials.

Biodegradable films composed of chitosan (3% *w/v*) and loaded with rosehip seed oil showed similar behavior. Although these films exhibited higher mechanical parameter values, the trend was the same. The films containing essential oil displayed an elongation at break of 11.7%, a value significantly higher than that of the control film (1.05%). The authors attributed this behavior to the plasticizing effect of the essential oil, which weakens intermolecular chain-to-chain interactions, leading to more flexible materials [27]. Pectin-based films (0.5%) enriched with limonene essential oil and stabilized with either nanocellulose or Tween 80 showed the same trend. Both materials, pectin/limonene/nanocellulose (65.87%) and pectin/limonene/Tween 80 (48.20%), exhibited a significant increase in elasticity compared to the control (23.94%) [50].

The addition of PO also affected the barrier properties. The water vapor permeability (WVP) of the films varied significantly with the inclusion of PO. WVP decreased as the essential oil concentration increased, reaching the lowest value in the film containing 1.5% PO (κ-1.5PO). Moeni et al. [58], suggest that adding hydrophobic ingredients (oil and lipids) to starch-based films reduces the WVP. This result can be attributed to the PO's lipophilic nature which repels water–matrix interactions, hindering permeation. Thus, materials that restrict this passage play an essential role in preserving packaged food by slowing down degradation reactions [59].

Xi Zhou et al. [60] developed biodegradable films based on konjac glucomannan (0.5%) and κ-carrageenan (0.5%) containing camellia oil (2, 4, and 6% *w/v*). The films exhibited the same behavior. The camellia oil-loaded materials showed lower water vapor permeability than control. The film containing 2% oil reduced permeability by approximately 45%. The authors attributed this result to the increased tortuosity factor of the vapor diffusion path through the films after the addition of oil. Another study also reported a reduction in water vapor permeability in corn starch films (2.5% w/v) loaded with soybean oil stabilized by bacterial nanocellulose (2.5, 5.0, and 7.5% *v*/v). The material containing 2.5% oil reduced permeability by 78% compared to the control. This effective result was attributed to the uniform dispersion of oil droplets within the film matrix and to the nature of the oil used in the emulsion [61].

3.7. Moisture content, swelling degree, and oil permeability

Measures of moisture content, swelling, contact angle, and oil permeability tests are displayed in Table 3. Moisture values ranged from 17.2 to 20.3%. The κ-0PO formulation showed the highest moisture content, followed by κ-0.5PO and κ-1.0PO/κ-1.5PO. This result was expected due to the hydrophilic nature of the κ-carrageenan/starch matrix. In contrast, the addition of PO, a hydrophobic material, tends to repel water molecules. These findings are consistent with the swelling test. An apparent reduction in water affinity was observed in the PO-loaded films. While the κ-0PO film showed swelling above 350%, those enriched with PO did not exceed 280%.

Finally, oil permeability values ranged from 0.04 to 0.39 g × mm × m^{-2} × d^{-1}. Although the molecules involved differ in size and polarity, both water vapor permeability (Table 2) and oil permeability followed similar trends. In both analyses, the κ-0.5PO formulation exhibited the lowest barrier to fluid and vapor transmission. Therefore, it can be

Table 3
Moisture content, swelling degree, and oil permeability of the κ-carrageenan/starch films.

Analysis	κ-0PO	κ-0.5PO	κ-1.0PO	κ-1.5PO
Moisture content (%)	20.14 ± 1.81^{a}	19.37 ± 1.85^{b}	17.02 ± 0.63^{cd}	17.32 ± 2.00^{c}
Swelling Degree (%)	357.86 ± 54.80^{a}	220.09 ± 1.79^{cd}	280.26 ± 27.9^{b}	227.19 ± 8.68^{c}
Oil Permeability (g × mm × m^{-2} × d^{-1})	0.33 ± 0.12^{b}	0.39 ± 0.04^{a}	0.07 ± 0.02^{c}	0.04 ± 0.01^{c}

Results are presented in (mean ± standard deviation); $n = 3$. a, b, c, d Different letters in the same row indicate significant differences ($p \leq 0.05$) according to Tukey's test.

Table 4
Color parameters, opacity and UV-barrier of the κ-carrageenan/starch films.

Films	κ-0PO	κ-0.5PO	κ-1PO	κ-1.5PO
L*	83.39 ± 0.74^{a}	81.13 ± 0.13^{b}	77.87 ± 0.56^{c}	77.01 ± 0.78^{cd}
a*	−0.48 ± 0.09^{d}	−7.51 ± 0.09^{bc}	−8.77 ± 0.19^{a}	−7.84 ± 0.64^{b}
b*	4.53 ± 0.35^{d}	33.02 ± 0.64^{c}	55.27 ± 0.59^{b}	59.47 ± 0.18^{a}
WI	82.77 ± 0.71^{a}	61.23 ± 0.50^{b}	39.82 ± 0.58^{c}	35.75 ± 0.27^{d}
Yi	7.74 ± 0.60^{d}	58.05 ± 1.05^{c}	101.21 ± 1.37^{b}	110.13 ± 1.20^{a}
ΔE	14.42 ± 0.72^{d}	36.07 ± 0.52^{c}	57.65 ± 0.58^{b}	61.73 ± 0.26^{a}
Opacity	0.96 ± 0.01^{d}	1. 13 ± 0.01^{c}	1.23 ± 0.00^{b}	1.24 ± 0.29^{a}
UV-Barrier (T_{280}%)	42.51 ± 0.07^{a}	28.55 ± 0.45^{b}	8.13 ± 0.19^{c}	6.18 ± 0.33^{d}

Results presented as (x ± SD); $n = 3$. L*: Brightness/brightness, a*; Redness/green, b*; Yellowness/blue; ΔE: color change; WI whiteness index; Opacity: Yi, yellowness index; Apparent opacity evaluated at 550 nm.
a, b, c Different letters in the same line indicate significant differences ($p \leq 0.05$) according to Tukey's test.

inferred that the internal structure of the material, before and after active incorporation, governs permeation behavior. In line with earlier study, oil permeability performance is attributed to the material's surface and internal structural properties [62].

3.8. Optical properties

The optical properties of the material were determined from color, opacity, and UV barrier measurements (Table 4). Color patterns were estimated using the parameters lightness/brightness (L), redness/greenness (a), yellowness/blueness (b), whiteness index (WI), yellowness index (Yi), and total color difference (ΔE). The control film (κ-0PO) was colorless and transparent, unlike the PO-loaded formulations. The ΔE parameter highlights this result. In addition, the PO-containing films exhibited a slightly yellowish color and higher opacity ($p \leq 0.05$). The parameter values a, Yi, and opacity confirm this observation. According to previous studies, the lipid phase can induce structural disorder within the material, creating voids at the film interface that lead to light scattering [63–65].

In addition to its slightly yellowish color, the essential oil also blocks part of the ultraviolet radiation incident on the material. A reduction in UV light transmittance is evident as PO concentration increases in the blend. The formulation containing 1.5% PO (κ-1.5PO) showed the best performance, followed by κ-1.0PO and κ-0.5PO ($p \leq 0.05$). These significant results are attributed to the minor components present in PO. Among them, carotenoids, compounds with conjugated double bonds, can absorb radiation in this range and reduce UV-induced lipid oxidation, thereby extending the shelf life of the packaged product [66].

3.9. Total carotenoid content

As discussed in Section 3.3, the carotenoids present in PO are responsible for the protective activity of the additive. Thus, the total carotenoid content in the films was determined by spectrophotometric measurements at 450 nm. The total carotenoid content ranged from 0.05 to 1.21 g/100 g of sample. The highest concentrations were observed in the κ-1.0PO (1.21 g/100 g sample) and κ-1.5PO (1.01 g/100 g of sample), followed by κ-0.5PO (0.43 g/100 g sample). The presence of the active compound in the packaging acts as an ultraviolet filter, preventing the passage of UV radiation that can accelerate oxidative processes in packaged foods, especially those rich in lipids [59]. Active starch-based packaging (4% *w/v*) loaded with palm oil extract (0–1.0%) and plasticized with glycerol extended the shelf life of butter by reducing lipid oxidation. The authors attributed this effect to the presence of carotenoids in PO [67].

Although κ-carrageenan and cassava starch films have been widely explored, this study introduces the incorporation of palm oil (active ingredient rich in carotenoids). The addition enables the development of an innovative polysaccharide–lipid system. The resulting matrix shows simultaneous improvements in mechanical strength and in water and light barrier properties.

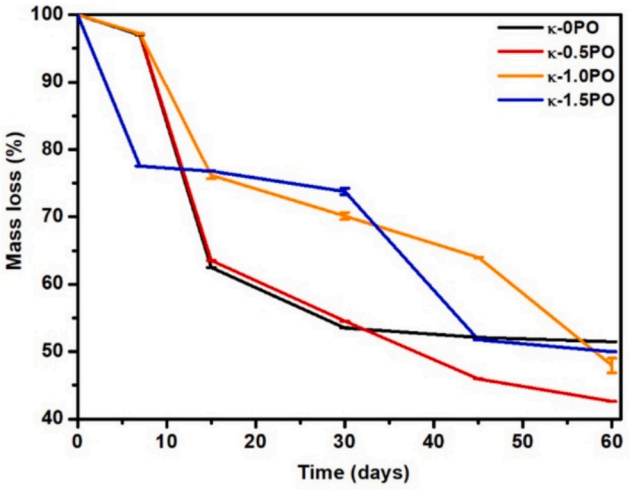

Fig. 7. Biodegradability test of the κ-carrageenan/starch films.

3.10. Biodegradability test

The biodegradability test of the films was conducted over 60 days. Material degradation was monitored by measuring mass loss during exposure (Fig. 7). All samples, including the control, were tested. Notably, all materials showed more than 50% mass loss within 60 days. The degradation occurs due to enzymatic attack on the glycosidic bonds of the polysaccharides that compose the film [68]. It can also be accelerated by edaphoclimatic factors such as temperature, pH, moisture, and soil nutrients [69,70]. The cleavage of these bonds produces low–molecular–weight saccharides, enabling the degradation process [4,71,72]. These findings highlight the importance of using environmentally friendly technologies. In addition to protecting and reducing food waste, the material is easily degraded by natural environmental action.

Similar results have been reported recently. Biodegradable films based on arrowroot starch (8% *w/v*), enriched with cinnamon essential oil and stabilized with pectin, showed more than 50% degradation after 21 days of testing. The authors noted that, although the material contained an antimicrobial active compound, it did not interfere with the enzymatic breakdown of starch molecules [68]. Arifin et al. developed a starch-based bionanocomposite film (3% w/v) reinforced with nanocellulose (0.5% w/v) and loaded with virgin coconut oil. The biodegradability results showed more than 60% degradation of the films [72].

3.11. Performance of the active coating on fresh tomato

The performance of the active films was evaluated as coatings on cherry tomatoes. The test was conducted using uncoated tomatoes, tomatoes coated with the control film (κ-0PO), and tomatoes coated with

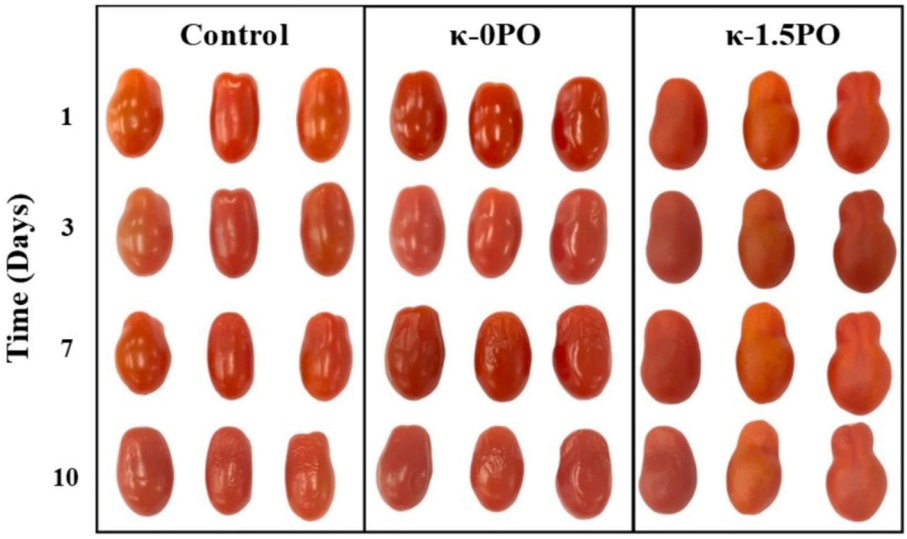

Fig. 8. Digital images of the tomato with/without coating for 10 days.

Table 5
Physicochemical analysis of the cherry tomato during the storage.

Analysis		Time (days)			
Mass Loss (%)	Treatment	1	3	7	10
	Control	16.77 ± 0.68^{bA}	16.45 ± 0.71^{cA}	15.69 ± 0.78^{cB}	15.33 ± 0.81^{bB}
	κ-0PO	19.02 ± 1.29^{aA}	18.45 ± 1.19^{aAB}	17.63 ± 1.04^{bB}	17.22 ± 0.96^{abB}
	κ-1.5PO	19.92 ± 1.43^{aA}	19.51 ± 1.44^{aA}	18.28 ± 1.36^{aB}	18.28 ± 0.30^{aB}
Titratable acidity	Control	1.69 ± 0.04^{cA}	1.58 ± 0.04^{cB}	1.52 ± 0.04^{aC}	1.30 ± 0.04^{bcD}
	κ-0PO	1.90 ± 0.04^{bA}	1.77 ± 0.10^{bB}	1.26 ± 0.10^{cC}	1.26 ± 0.13^{bC}
	κ-1.5PO	2.39 ± 0.07^{aA}	2.11 ± 0.1^{aB}	1.39 ± 0.07^{bC}	1.39 ± 0.10^{aC}
pH	Control	4.31 ± 0.01^{b}	4.31 ± 0.02^{cC}	4.36 ± 0.02^{cB}	4.46 ± 0.03^{bA}
	κ-0PO	4.26 ± 0.04^{bcC}	4.41 ± 0.01^{aB}	4.40 ± 0.02^{abB}	4.52 ± 0.04^{aA}
	κ-1.5PO	4.35 ± 0.03^{aC}	4.40 ± 0.01^{aB}	4.42 ± 0.02^{aA}	4.42 ± 0.02^{cA}

a, b, c, d Different letters in the same column indicate significant differences ($p \leq 0.05$) between days according to the Tukey test.
A, B, C, D Different letters in the same line indicate significant differences ($p \leq 0.05$) between the groups according to the Tukey test.

the κ-1.5PO formulation, all stored under controlled temperature (25 ± 0.5 °C). The fruits were monitored through digital imaging (Fig. 8) and physicochemical analyses (weight loss, titratable acidity, and *p*H; Table 5) at four sampling points over 10 days. The active coating maintained the tomatoes' appearance throughout the ten-day experiment (Fig. 8). In contrast, the control-coated and uncoated fruits showed visible signs of degradation during the same period. This finding highlights the protective effect attributed to palm oil.

The mass loss results corroborate with the positive performance of the PO-loaded coating. Tomatoes coated with active material showed the lowest mass loss ($p \leq 0.05$). Reduced gas exchange between the fruit and the environment contributed to the formulation's improved performance. The lowest WVP results (Table 2) exhibited by κ-1.5PO support these findings.

During ripening, synthesis and degradation reactions (including ethylene and respiration metabolism) occur, leading to changes in the fruit's physicochemical properties [45]. For example, the degradation of organic acids during ripening influences titratable acidity and increases pH [73]. Therefore, minor *p*H variations during storage favor a longer shelf life for the fruit. These findings reinforce the active coating's positive performance, which showed the lowest *p*H variation among the treatments ($\Delta pH = -0.07$). Thus, preserving the quality of fruits and vegetables during storage is essential. In addition to reducing waste, it has a positive impact on the entire production chain involved [74].

4. Conclusion

The addition of 1.5% palm oil (PO) to the starch/κ-carrageenan film matrix induced changes in the physicochemical, mechanical, optical, and permeability properties of the material. The results indicate that PO modified the film's internal structure, which improved the mechanical strength and water-vapor barrier properties. Furthermore, the presence of carotenoids in PO enabled the active material to block ultraviolet radiation, thereby extending the shelf life of cherry tomatoes. The biodegradable nature of the packaging was confirmed through biodegradation tests, which demonstrated a mass loss exceeding 50% after 60 days. In conclusion, new active, biodegradable packaging materials were developed, characterized, and applied, showing a significant effect on extending the shelf life of fresh tomatoes.

However, the negative point is the cost of development. Based on laboratory-scale calculations, the estimated raw material cost of the developed starch–κ-carrageenan coating is approximately $ 3.89–4.28/m^2 (100–160 μm thickness). For comparison, Polylactic Acid (PLA, a synthetic and biodegradable polymer) presents an estimated raw material cost of $ 0.16–0.42/m^2, without active compounds. The incorporation of antioxidants increases this value due to additional material and processing costs. Conventional polyethylene (PE, a synthetic and non-biodegradable polymer) is substantially cheaper. PE packaging costs approximately $ 0.05–0.16/m^2. The significantly lower cost of PE is mainly due to its fully consolidated petrochemical production chain, very large industrial scale, and decades of process optimization. In contrast, biodegradable and active films are produced on a smaller scale

and target higher value-added sustainable markets.

CRediT authorship contribution statement

Joice Camila Martins da Costa: Writing – original draft, Visualization, Methodology, Investigation, Formal analysis, Data curation, Conceptualization. **Eloize da Silva Alves:** Methodology, Formal analysis. **Talita Aparecida Ferreira de Campos:** Writing – review & editing, Formal analysis. **Johny Paulo Monteiro:** Writing – original draft, Formal analysis, Data curation. **João Carlos Martins da Costa:** Writing – original draft, Formal analysis. **Alessandro Francisco Martins:** Writing – review & editing, Visualization, Investigation, Data curation. **Tatiana La Banca Schreiner:** Writing – review & editing, Visualization, Investigation, Formal analysis. **Maria Filomena Filipe Barreiro:** Writing – review & editing. **Elton Guntendorfer Bonafe:** Writing – review & editing, Supervision, Resources, Project administration, Conceptualization.

Declaration of competing interest

The authors declare that they have no known competing financial interests or personal relationships that could have appeared to influence the work reported in this paper.

Acknowledgements

The authors gratefully acknowledge the financial support provided by the Coordination for the Improvement of Higher Education Personnel (CAPES) and the National Council for Scientific and Technological Development (CNPq, Grant numbers: 314046/2023-2 and 409889/2023-7). We also thank the Universidade Estadual de Maringá (Complexo de Centrais de Apoio à Pesquisa – COMCAP), the multi-user research support laboratory at the Universidade Tecnológica Federal do Paraná (UTFPR) (LAMAP), the Universidade do Estado do Amazonas (Centro Multiusuário para Análise de Fenômenos Biomédicos - CMA-Bio), and the Instituto Federal do Amazonas (Campus Manaus Distrito Industrial - CMDI) for their partnership and support during the analyses. Foundation for Science and Technology (FCT, Portugal) for financial support via national funds FCT/MCTES (PIDDAC) to CIMO UID/00690/2025 (10.54499/UID/00690/2025) and UID/PRR/00690/2025 (10.54499/UID/PRR/00690/2025); and SusTEC, LA/P/0007/2020 (DOI: 10.54499/LA/P/0007/2020). The authors thank the Tate & Lyle for polysaccharideś donation.

Data availability

No data was used for the research described in the article.

References

[1] X. Dang, Y. Cai, X. Wang, An all-natural strategy for versatile biomass-based active food packaging film with superior biodegradability, antioxidant and antimicrobial activity, Food Chem. 480 (2025) 143922, https://doi.org/10.1016/j.foodchem.2025.143922.

[2] S. Wei, Y. Sun, L. Zhao, X. Li, J. Xue, From wastes to functional materials: preparation, modification, and applications of polysaccharide-based biodegradable films, Carbohydr. Polym. 368 (2025), https://doi.org/10.1016/j.carbpol.2025.124230.

[3] X. Dang, S. Han, Y. Du, Y. Fei, B. Guo, X. Wang, Engineered environment-friendly multifunctional food packaging with superior nonleachability, polymer miscibility and antimicrobial activity, Food Chem. 466 (2025) 142192, https://doi.org/10.1016/j.foodchem.2024.142192.

[4] G.A.M. Jesus, M.C. Castro, P.R. Souza, J.P. Monteiro, R.M. Sabino, S.S. Sablani, A. F. Martins, E.G. Bonafé, Antioxidant, UV-blocking, and biodegradable pectin films containing selenium nanoparticles for sustainable food packaging, Food Hydrocoll. 167 (2025) 111449, https://doi.org/10.1016/j.foodhyd.2025.111449.

[5] R. Kraisitthisirintr, W. Choeybandit, T. Karbowiak, S. Wongwat, N. Suntipabvivattana, P. Kaewprachu, P. Rachtanapun, K. Jantanasakulwong, Asadullah, D. Noiwan, W. Tongdeesoontorn, Biodegradable planting bags composed of a biocomposite film using cassava starch and soy protein isolate: design, production, and application, Environ. Technol. Innov. 39 (2025) 104299, https://doi.org/10.1016/j.eti.2025.104299.

[6] Z. Liu, M. Yang, L. Hu, J. Xu, F. Wang, L. Liu, J. Kang, Biodegradable active films developed from low-methoxyl pectin incorporated with cellulose nanocrystals-stabilized oregano essential oil Pickering emulsions, Int. J. Biol. Macromol. 328 (2025), https://doi.org/10.1016/j.ijbiomac.2025.147127.

[7] M.L.C. Chaves, G.A.M. Jesus, M.C. Castro, A.R.S. Bruni, J.P. Monteiro, O. O. SantosJunior, A.F. Martins, E.G. Bonafé, Biodegradable pectin/starch-based films applied on fresh pears, ACS Omega 10 (2025) 24050–24062, https://doi.org/10.1021/acsomega.4c08591.

[8] J.P. de Oliveira, V. de Souza Moreira, J.S. de Oliveira, L.B. Landim, N.M.C. da Silva, C.P. de Oliveira, Development and characterization of biodegradable active films based on rice starch with nanocellulose and Amaranthus viridis extract, Int. J. Biol. Macromol. 318 (2025) 145243, https://doi.org/10.1016/j.ijbiomac.2025.145243.

[9] X. Dang, S. Han, X. Wang, Versatile corn starch-based sustainable food packaging with enhanced antimicrobial activity and preservative properties, J. Colloid Interface Sci. 694 (2025) 137698, https://doi.org/10.1016/j.jcis.2025.137698.

[10] T. Jiang, Q. Duan, J. Zhu, H. Liu, L. Yu, Starch-based biodegradable materials: challenges and opportunities, Adv. Ind. Eng. Polym. Res. 3 (2020) 8–18, https://doi.org/10.1016/j.aiepr.2019.11.003.

[11] J.C.M. da Costa, A.R.S. Bruni, G.A.M. Jesus, E.S. Alves, O. de Oliveira S. Júnior, A. F. Martins, E.G. Bonafe, Enhancing fresh pear preservation with UV-blocking film coatings based on κ-carrageenan, cassava starch, and copper oxide particles, J. Food Eng. 368 (2024), https://doi.org/10.1016/j.jfoodeng.2023.111853.

[12] C. de Lima Barizão, M.I. Crepaldi, O. de O.S. Junior, A.C. de Oliveira, A.F. Martins, P.S. Garcia, E.G. Bonafé, Biodegradable films based on commercial κ-carrageenan and cassava starch to achieve low production costs, Int. J. Biol. Macromol. 165 (2020) 582–590, https://doi.org/10.1016/j.ijbiomac.2020.09.150.

[13] Z. Cheng, Y. Qiu, M. Bian, Y. He, S. Xu, Y. Li, I. Ahmad, Y. Ding, F. Lyu, Muscle fibrous structural design of plant-based meat analogs: advances and challenges in 3D printing technology, Trends Food Sci. Technol. 147 (2024) 104417, https://doi.org/10.1016/j.tifs.2024.104417.

[14] Q. Lin, Y. Hu, C. Qiu, X. Li, S. Sang, D.J. McClements, L. Chen, J. Long, X. Xu, J. Wang, Z. Jin, Peanut protein-polysaccharide hydrogels based on semi-interpenetrating networks used for 3D/4D printing, Food Hydrocoll. 137 (2023) 108332, https://doi.org/10.1016/j.foodhyd.2022.108332.

[15] D.M.C. Marques, J.C. Silva, A.P. Serro, J.M.S. Cabral, P. Sanjuan-Alberte, F. C. Ferreira, 3D bioprinting of novel κ-carrageenan bioinks: An algae-derived polysaccharide, Bioengineering 9 (2022) 109, https://doi.org/10.3390/bioengineering9030109.

[16] R. Balasubramanian, S.S. Kim, J. Lee, Novel synergistic transparent k-carrageenan/xanthan gum/Gellan gum hydrogel film: mechanical, thermal and water barrier properties, Int. J. Biol. Macromol. 118 (2018) 561–568, https://doi.org/10.1016/j.ijbiomac.2018.06.110.

[17] R. Gheorghita (Puscaselu), G. Gutt, S. Amariei, The use of edible films based on sodium alginate in meat product packaging: an eco-friendly alternative to conventional plastic materials, Coatings 10 (2020) 166, https://doi.org/10.3390/coatings10020166.

[18] S. Taylor, A. Colonna, J. Jung, J. Gutierrez, Y. Zhao, Consumer perception and acceptance of edible packaging for various food products, J. Food Sci. 89 (2024) 2423–2437, https://doi.org/10.1111/1750-3841.16992.

[19] B. Kokkuvayil Ramadas, J.-W. Rhim, S. Roy, Recent Progress of carrageenan-based composite films in active and intelligent food packaging applications, Polymers (Basel). 16 (2024) 1001, https://doi.org/10.3390/polym16071001.

[20] N. Oladzadabbasabadi, S. Ebadi, A. Mohammadi Nafchi, A.A. Karim, S. R. Kiahosseini, Functional properties of dually modified sago starch/κ-carrageenan films: An alternative to gelatin in pharmaceutical capsules, Carbohydr. Polym. 160 (2017) 43–51, https://doi.org/10.1016/j.carbpol.2016.12.042.

[21] C. Wang, Y. Lu, Z. Li, X. An, Z. Gao, S. Tian, Preparation and performance characterization of a composite film based on corn starch, κ-carrageenan, and ethanol extract of onion skin, Polymers (Basel). 14 (2022) 2986, https://doi.org/10.3390/polym14152986.

[22] M.A. Cerqueira, B.W.S. Souza, J.A. Teixeira, A.A. Vicente, Effect of glycerol and corn oil on physicochemical properties of polysaccharide films – a comparative study, Food Hydrocoll. 27 (2012) 175–184, https://doi.org/10.1016/j.foodhyd.2011.07.007.

[23] L. Stoll, R. Rech, S.H. Flôres, S.M.B. Nachtigall, A. de Oliveira Rios, Poly(acid lactic) films with carotenoids extracts: release study and effect on sunflower oil preservation, Food Chem. 281 (2019) 213–221, https://doi.org/10.1016/j.foodchem.2018.12.100.

[24] J.G. de Oliveira Filho, M.R.V. Bertolo, M.Á.V. Rodrigues, G. da C. Silva, G.M.N. de Mendonça, S. Bogusz Junior, M.D. Ferreira, M.B. Egea, Recent advances in the development of smart, active, and bioactive biodegradable biopolymer-based films containing betalains, Food Chem. 390 (2022) 133149, https://doi.org/10.1016/j.foodchem.2022.133149.

[25] D.O. Edem, Palm oil: biochemical, physiological, nutritional, hematological and toxicological aspects: a review, Plant Foods Hum. Nutr. 57 (2002) 319–341, https://doi.org/10.1023/A:1021828132707.

[26] S. Nurul Syahida, M.R. Ismail-Fitry, Z.M.A. Ainun, Z.A. Nur Hanani, Effects of palm wax on the physical, mechanical and water barrier properties of fish gelatin films for food packaging application, Food Packag. Shelf Life 23 (2020) 100437, https://doi.org/10.1016/j.fpsl.2019.100437.

[27] E. Butnaru, E. Stoleru, M.A. Brebu, R.N. Darie-Nita, A. Bargan, C. Vasile, Chitosan-based bionanocomposite films prepared by emulsion technique for food preservation, Materials 12 (2019), https://doi.org/10.3390/ma12030373.

[28] A.P. Lopes, P.R. Souza, E.G. Bonafé, J.V. Visentainer, A.F. Martins, E.A. Canesin, Purified glycerol is produced from the frying oil transesterification by combining a pre-purification strategy performed with condensed tannin polymer derivative followed by ionic exchange, Fuel Process. Technol. 187 (2019) 73–83, https://doi.org/10.1016/J.FUPROC.2019.01.014.
[29] A.R. da Silva Bruni, J. de Souza Alves Friedrichsen, G.A.M. de Jesus, E. da Silva Alves, J.C.M. da Costa, P.R. Souza, O. de Oliveira Santos Junior, E.G. Bonafe, Characterization and application of active films based on commercial polysaccharides incorporating ZnONPs, Int. J. Biol. Macromol. 224 (2023) 1322–1336, https://doi.org/10.1016/j.ijbiomac.2022.10.219.
[30] L. Del, C.B. Araújo, H.K. De Matos, P. Facchi, A. De Almeida, B.M.G. Gonçalves, J. P. Monteiro, A.F. Martins, E.G. Bonafe, natural carbohydrate-based thermosensitive chitosan / pectin adsorbent for removal of Pb (II) from aqueous solutions, Int. J. Biol. Macromol. 193 (2021) 1813–1822.
[31] G.A.M. de Jesus, S.B.R. Berton, B.M. Simões, R.S. Zola, J.P. Monteiro, A.F. Martins, E.G. Bonafé, K-Carrageenan/poly(vinyl alcohol) functionalized films with gallic acid and stabilized with metallic ions, Int. J. Biol. Macromol. 253 (2023) 127087, https://doi.org/10.1016/j.ijbiomac.2023.127087.
[32] S.B.R. Berton, G.A.M. de Jesus, R.M. Sabino, J.P. Monteiro, S.A.S. Venter, M. L. Bruschi, K.C. Popat, M. Matsushita, A.F. Martins, E.G. Bonafé, Properties of a commercial κ-carrageenan food ingredient and its durable superabsorbent hydrogels, Carbohydr. Res. 487 (2020) 107883, https://doi.org/10.1016/j.carres.2019.107883.
[33] J.H. Jagannath, C. Nanjappa, D. Das Gupta, A.S. Bawa, Studies on the stability of an edible film and its use for the preservation of carrot (*Daucus carota*), Int. J. Food Sci. Technol. 41 (2006) 498–506, https://doi.org/10.1111/j.1365-2621.2005.01038.x.
[34] A.R. da Silva Bruni, E. da Silva Alves, J.C.M. da Costa, J. de S.A. Friedrichsen, L.G. Z. Silva, O. de Oliveira Santos Junior, E.G. Bonafé, Extending the postharvest shelf life of strawberries through a κ-carrageenan/starch-based coating enriched with zinc oxide nanoparticles, ACS Food Sci. Technol. 4 (2024) 2967–2979, https://doi.org/10.1021/acsfoodscitech.4c00574.
[35] J.S.A. Friedrichsen, A.R.S. Bruni, E.S. Alves, B.H.F. Saqueti, A.L. Figueiredo, P. R. de Souza, J.M.G. Mikcha, M.R.S. Scapim, E.G. Bonafe, O.O. Santos, Biodegradable coatings based on cassava starch and poly(vinyl alcohol): potential application for prolonging the shelf life of strawberries (Fragaria ananassa) cv. San Andreas, ACS Food Sci. Technol. 4 (2024) 365–372, https://doi.org/10.1021/acsfoodscitech.3c00456.
[36] C.R. Rech, K.C. da Silva Brabes, B.E. Bagnara e Silva, P.R.S. Bittencourt, M. T. Koschevic, T.F.S. da Silveira, M.A.U. Martines, T. Caon, S.M. Martelli, Biodegradation of eugenol-loaded polyhydroxybutyrate films in different soil types, Case Stud. Chem. Environ. Eng. 2 (2020), https://doi.org/10.1016/j.cscee.2020.100014.
[37] T. Karbowiak, F. Debeaufort, D. Champion, A. Voilley, Wetting properties at the surface of iota-carrageenan-based edible films, J. Colloid Interface Sci. 294 (2006) 400–410, https://doi.org/10.1016/j.jcis.2005.07.030.
[38] K. Schroën, J. de Ruiter, C. Berton-Carabin, The importance of interfacial tension in emulsification: connecting scaling relations used in large scale preparation with microfluidic measurement methods, ChemEngineering 4 (2020) 1–22, https://doi.org/10.3390/chemengineering4040063.
[39] M. L'Estimé, M. Schindler, N. Shahidzadeh, D. Bonn, Droplet size distribution in emulsions, Langmuir 40 (2024) 275–281, https://doi.org/10.1021/acs.langmuir.3c02463.
[40] S.P. Patil, S.A. Bhalerao, Y.N. Rajput, A.P. Pratap, Production of Rhamnolipids using WFSO and its application in the development of antifungal nanoemulsion using Hydnocarpus Wightiana, Garcinia Cambogia - seed oils, Ind. Crop. Prod. 219 (2024) 118885, https://doi.org/10.1016/j.indcrop.2024.118885.
[41] Ü. Erdoğan, E.H. Gökçe, Fig seed oil-loaded nanostructured lipid carriers: evaluation of the protective effects against oxidation, J. Food Process. Preserv. 45 (2021), https://doi.org/10.1111/jfpp.15835.
[42] D.C. Rodrigues, A.P. Cunha, E.S. Brito, H.M.C. Azeredo, M.I. Gallão, Mesquite seed gum and palm fruit oil emulsion edible films: influence of oil content and sonication, Food Hydrocoll. 56 (2016) 227–235, https://doi.org/10.1016/j.foodhyd.2015.12.018.
[43] W.J. do Nascimento, J.C.M. da Costa, E.S. Alves, M.C. de Oliveira, J.P. Monteiro, P. R. Souza, A.F. Martins, E.G. Bonafe, Zinc oxide nanoparticle-reinforced pectin/starch functionalized films: a sustainable solution for biodegradable packaging, Int. J. Biol. Macromol. 257 (2024), https://doi.org/10.1016/j.ijbiomac.2023.128461.
[44] P. Fatehi, A.S. Baba, V.R. Eh suk, M. Misran, Preparation and characterization of palm oil in water microemulsion for application in the food industry, Br. Food J. 122 (2020) 3077–3088, https://doi.org/10.1108/BFJ-01-2020-0018.
[45] K. Sivasankar, A. Pathak, K. Jain, Effect of tween 80 and Pluronic 127 on the stabilization of zein nanocarriers for the delivery of piperine, Food Res. Int. 197 (2024), https://doi.org/10.1016/j.foodres.2024.115202.
[46] X. Li, Z. Tu, X. Sha, Y. Ye, Z. Li, Flavor, antimicrobial activity, and physical properties of composite film prepared with different surfactants, Food Sci. Nutr. 8 (2020) 3099–3109, https://doi.org/10.1002/fsn3.1526.
[47] S.N.H. Mustapha, M.N. Md Nizam, M.I. Mohamad Isa, R. Roslan, R. Mustapha, Synthesis and characterization of hydrophobic properties of silicon dioxide in palm oil based bio-coating, Mater. Today Proc. 51 (2022) 1415–1419, https://doi.org/10.1016/j.matpr.2021.11.636.
[48] D.C. Rodrigues, A.P. Cunha, E.S. Brito, H.M.C. Azeredo, M.I. Gallão, Mesquite seed gum and palm fruit oil emulsion edible films: influence of oil content and sonication, Food Hydrocoll. 56 (2016) 227–235, https://doi.org/10.1016/j.foodhyd.2015.12.018.
[49] P. Tongnuanchan, S. Benjakul, T. Prodpran, K. Nilsuwan, Emulsion film based on fish skin gelatin and palm oil: physical, structural and thermal properties, Food Hydrocoll. 48 (2015) 248–259, https://doi.org/10.1016/j.foodhyd.2015.02.025.
[50] G. Kusuma, V. Marcellino, A.A. Wardana, L.P. Wigati, C. Liza, R. Wulandari, R.H. B. Setiarto, F. Tanaka, F. Tanaka, W. Ramadhan, Biofunctional features of Pickering emulsified film from citrus peel pectin/limonene oil/nanocrystalline cellulose, Int. J. Food Sci. Technol. 59 (2024) 7837–7851, https://doi.org/10.1111/ijfs.17049.
[51] J. Ng, S.Y. Lee, Y.Y. Thoo, Gellan gum film incorporated with palm kernel oil Nanoemulsion for enhanced barrier properties, Food Biophys. 20 (2025), https://doi.org/10.1007/s11483-025-09956-9.
[52] J.S. Lee, E. sil Lee, J. Han, Enhancement of the water-resistance properties of an edible film prepared from mung bean starch via the incorporation of sunflower seed oil, Sci. Rep. 10 (2020), https://doi.org/10.1038/s41598-020-70651-5.
[53] A.A. Shamsuri, S.N.A.Md. Jamil, Functional properties of biopolymer-based films modified with surfactants: a brief review, Processes 8 (2020) 1039, https://doi.org/10.3390/pr8091039.
[54] P. Tongnuanchan, S. Benjakul, T. Prodpran, Structural, morphological and thermal behaviour characterisations of fish gelatin film incorporated with basil and citronella essential oils as affected by surfactants, Food Hydrocoll. 41 (2014) 33–43, https://doi.org/10.1016/j.foodhyd.2014.03.015.
[55] M. Zhang, H. Chen, Development and characterization of starch-sodium alginate-montmorillonite biodegradable antibacterial films, Int. J. Biol. Macromol. 233 (2023) 123462, https://doi.org/10.1016/j.ijbiomac.2023.123462.
[56] O.G. Piringer, A.L. Baner, Platic Packaging: Interactions with Food and Pharmaceuticals, 2008.
[57] X. Wang, J. Huang, Y. Zhang, H. Zeng, W. Li, Y. Wang, Design and application of antibacterial bioactive films for food preservation: a review, J. Agric. Food Chem. 73 (2025) 19244–19261, https://doi.org/10.1021/acs.jafc.5c05959.
[58] A. Moeini, P. Pedram, E. Fattahi, P. Cerruti, G. Santagata, Edible polymers and secondary bioactive compounds for food packaging applications: antimicrobial, mechanical, and gas barrier properties, Polymers (Basel). 14 (2022) 2395, https://doi.org/10.3390/polym14122395.
[59] S. Roy, R.K. Deshmukh, S. Tripathi, K.K. Gaikwad, S.S. Das, D. Sharma, Recent advances in the carotenoids added to food packaging films: a review, Foods 12 (2023) 4011, https://doi.org/10.3390/foods12214011.
[60] X. Zhou, X. Zong, S. Wang, C. Yin, X. Gao, G. Xiong, X. Xu, J. Qi, L. Mei, Emulsified blend film based on konjac glucomannan/carrageenan/ camellia oil: physical, structural, and water barrier properties, Carbohydr. Polym. 251 (2021) 117100, https://doi.org/10.1016/j.carbpol.2020.117100.
[61] N.T. de Almeida, A.L.S. Pereira, M. de Oliveira Barros, A.L.A. Mattos, M. de F. Rosa, Enhancing starch film properties using bacterial nanocellulose-stabilized Pickering emulsions, Polymers (Basel) 16 (2024), https://doi.org/10.3390/polym16233346.
[62] D. Lin, Y. Zheng, X. Wang, Y. Huang, L. Ni, X. Chen, Z. Wu, C. Huang, Q. Yi, J. Li, W. Qin, Q. Zhang, H. Chen, D. Wu, Study on physicochemical properties, antioxidant and antimicrobial activity of okara soluble dietary fiber/sodium carboxymethyl cellulose/thyme essential oil active edible composite films incorporated with pectin, Int. J. Biol. Macromol. 165 (2020) 1241–1249, https://doi.org/10.1016/j.ijbiomac.2020.10.005.
[63] M.J. Fabra, R. Pérez-Masiá, P. Talens, A. Chiralt, Influence of the homogenization conditions and lipid self-association on properties of sodium caseinate based films containing oleic and stearic acids, Food Hydrocoll. 25 (2011) 1112–1121, https://doi.org/10.1016/j.foodhyd.2010.10.008.
[64] B. Saberi, S. Chockchaisawasdee, J.B. Golding, C.J. Scarlett, C.E. Stathopoulos, Development of biocomposite films incorporated with different amounts of shellac, emulsifier, and surfactant, Food Hydrocoll. 72 (2017) 174–184, https://doi.org/10.1016/j.foodhyd.2017.05.042.
[65] C.U. López-Palestina, C.L. Aguirre-Mancilla, J.C. Raya-Pérez, J.G. Ramirez-Pimentel, A. Vargas-Torres, A.D. Hernández-Fuentes, Physicochemical and antioxidant properties of gelatin-based films containing oily tomato extract (*Solanum lycopersicum* L.), CyTA - J. Food 17 (2019) 142–150, https://doi.org/10.1080/19476337.2018.1564793.
[66] S.K. N, A.H. Dar, S. Srivastava, K.K. Dash, V.K. Pandey, Carotenoids based smart packaging: a comprehensive review, Measurement: Food 15 (2024) 100190, https://doi.org/10.1016/j.meafoo.2024.100190.
[67] K.K.N.C.L. Perazzo, A. Carlos De Vasconcelos Conceição, J.C. Pires Dos Santos, D. De Jesus Assis, C.O. Souza, J.I. Druzian, Properties and antioxidant action of actives cassava starch films incorporated with green tea and palm oil extracts, PLoS One 9 (2014), https://doi.org/10.1371/journal.pone.0105199.
[68] D. Mathew, N.M. Sudheep, B. Thomas, Cinnamon essential oil-enriched arrowroot starch-based biodegradable films for sustainable packaging and microbial preservation of chicken meat, Results Surf. Interfaces 20 (2025), https://doi.org/10.1016/j.rsurfi.2025.100617.
[69] J. Ge, W. Lu, H. Zhang, Y. Gong, J. Wang, Y. Xie, Q. Chang, X. Deng, Exploring sustainable food packaging: Nanocellulose composite films with enhanced mechanical strength, antibacterial performance, and biodegradability, Int. J. Biol. Macromol. 259 (2024) 129200, https://doi.org/10.1016/j.ijbiomac.2024.129200.
[70] S.A. El Mogy, R.M. Mourad, A. Abdel-Hakim, Characterization of biodegradable composite based on microalgae modified glycerol-plasticized-starch films, Polym. Eng. Sci. 64 (2024) 1168–1180, https://doi.org/10.1002/pen.26605.
[71] J. Li, C. Peng, A. Mao, M. Zhong, Z. Hu, An overview of microbial enzymatic approaches for pectin degradation, Int. J. Biol. Macromol. 254 (2024), https://doi.org/10.1016/j.ijbiomac.2023.127804.
[72] H.R. Arifin, Y.C. Angelica, B. Nurhadi, H. Marta, R.C. Nissa, Elephant foot yam starch-NCC bionanocomposite film incorporated with virgin coconut oil and

Monoglyceride for hydrophobic and biodegradable packaging, J. Renew. Mater. 13 (2025) 617–635, https://doi.org/10.32604/jrm.2025.057812.

[73] M.F. Almeida, G.L. Silva, G.D. Gondim, C.E.F. Alves, M.C. Silva, B. de Andrade Braga Mendes, D.A. dos Anjos, A.R. São José, C.M. Veloso, Maintenance of postharvest quality of 'palmer' mango coated with biodegradable coatings based on cassava starch and emulsion of lemongrass essential oil, Int. J. Biol. Macromol. 277 (2024) 134323, https://doi.org/10.1016/j.ijbiomac.2024.134323.

[74] M. Rasouli, M. Koushesh Saba, A. Ramezanian, Inhibitory effect of salicylic acid and Aloe vera gel edible coating on microbial load and chilling injury of orange fruit, Sci. Hortic. 247 (2019) 27–34, https://doi.org/10.1016/j.scienta.2018.12.004.